analytical chemistry

Article

pubs.acs.org/ac

Live Cell Integrated Surface Plasmon Resonance Biosensing Approach to Mimic the Regulation of Angiogenic Switch upon Anti-Cancer Drug Exposure

Chang Liu,[†] Subbiah Alwarappan,[‡] Haitham A. Badr,[§] Rui Zhang,[†] Hongyun Liu,[∥] Jun-Jie Zhu,[⊥] and Chen-Zhong Li*[,†]

[†]Nanobioengineering/Bioelectronics Laboratory, Department of Biomedical Engineering, Florida International University, Miami, Florida, 33174, United States

[‡]Bio-electrochemistry Research Group, CSIR-Central Electrochemical Research Institute, Karaikudi, Tamilnadu, 630006, India

[§]Department of Biochemistry, Faculty of Agriculture, Zagazig University, Zagazig, 44511, Egypt

[∥]College of Chemistry, Beijing Normal University, Beijing, China

[⊥]State Key Laboratory of Analytical Chemistry for Life Science, School of Chemistry and Chemical Engineering, Nanjing University, Nanjing, China

Supporting Information

ABSTRACT: In this work, we report a novel surface plasmon resonance (SPR) based live-cell biosensing platform to measure and compare the binding affinity of vascular endothelial growth factor (VEGF) to vascular endothelial growth factor receptor (VEGFR) and VEGF to bevacizumab. Results have shown that bevacizumab binds VEGF with a higher association rate and affinity compared to VEGFR. Further, this platform has been employed to mimic the *in vivo* condition of the VEGF−VEGFR angiogenic switch. Competitive binding to VEGF between VEGFR and bevacizumab was monitored in real-time using this platform. Results demonstrated a significant blockage of VEGF−VEGFR binding by bevacizumab. From the results, it is evident that the proposed strategy is simple and highly sensitive for the direct and real-time measurements of bevacizumab drug efficacy to the VEGF−VEGFR angiogenic switch in living SKOV-3 cells.

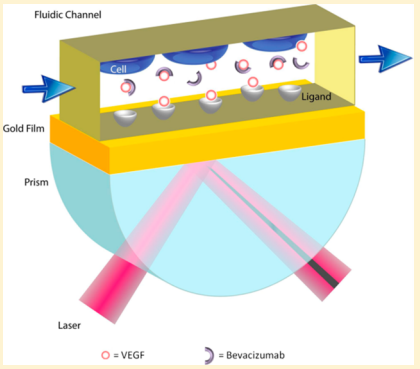

In the past decade, cancer has been reported as the second major cause of death in the United States.[1] Although there are several types of cancer, a common cause for any type of cancer is the abnormal growth of cells.[2−4] Further, very often, cancer cells form a tumor. A tumor larger than a millimeter will starve itself for oxygen and energy, unless new blood vessels are built to provide supplies. During such circumstances, a process known as angiogenesis is found to be involved in building new blood vessels for many types of cancer.[5] Angiogenesis is a complex process and is defined as the growth of new blood vessels from existing vessels.[6,7] Mediators of angiogenesis such as vascular endothelial growth factor (VEGF) stimulate endothelial cells to secrete proteases and plasminogen activators. Cells will then migrate, proliferate, and eventually differentiate to form a new lumen vessel.[8] Several pathological conditions involve or mimic the angiogenic process. Cancer switches on angiogenesis by breaking the balance between productions of angiogenic stimulus and inhibiting factors.[9,10] Vascular endothelial growth factor receptor (VEGFR) refers to a family of endothelial cell membrane receptors that bind with the VEGFs secreted by tumors. VEGF−VEGFR binding process is the key point of neovascularization.[11,12] Targeting the endothelial cells receptor binding and activation process is a promising strategy for cancer repression. However, there are several questions about the VEGF−VEGFR angiogenic switch including the binding kinetics remain unclear.

Despite the fact that there are several unanswered fundamental questions, biochemical therapies targeting angiogenic switches are rapidly emerging in the anticancer pharmaceutical industry. Further, the side effects associated with biochemical therapies are negligible upon comparison with chemotherapy and radiotherapy.[13] At present, FDA approved about 100 antibodies based cancer therapy for regulating the VEGF−VEGFR angiogenic switch.[14−16] One such approved antibody is bevacizumab, a humanized anti-VEGF monoclonal antibody generated by engineering the VEGF binding residues of a murine neutralizing antibody into the framework of the consensus human immunoglobulin G1 (IgG1).[17] Bevacizumab recognizes, binds and blocks all biologically active forms of VEGF that interact with VEGFRs.[18] The binding epitope of VEGF for bevacizumab has been determined structurally in a previous study: Fab domain of bevacizumab binding centers on

Received: August 21, 2013
Accepted: July 9, 2014
Published: July 9, 2014

Gly-88 residue of the human VEGF.[19] The efficacy of bevacizumab against various cancer types has been demonstrated in several clinical studies.[20−24] (Supporting Information, Table S1)

Although there are several clinical studies and trials on the drug efficacy of bevacizumab on cancers, only a few fundamental studies have been reported on the interaction between bevacizumab and VEGF.[25,26] A kinetics study on VEGF-bevacizumab binding is essential to elucidate the fundamental mechanism of bevacizumab inhibition to the VEGF−VEGFR angiogenic switch. Traditional biological techniques employed to measure the binding kinetics of VEGF and bevacizumab include Western Blot and ELISA.[27,28] These techniques measure biomolecular binding only at a single time point and therefore are not useful for real-time monitoring. Electrochemical biosensors provide continuous monitoring of biomolecular bindings. However, a labeling procedure is required in order to detect non redox-active analytes.[29,30] The recent rapid development of surface plasmon resonance (SPR) biosensors has offered an engineering solution to overcome these limitations. SPR offers highly sensitive label-free detection, and it is also a powerful tool for binding kinetic studies.[31−33] SPR transforms the refractive index change induced by biomolecular binding events on the sensing surface into the shift of the plasmon extinction wavelength. Real-time biomolecular binding kinetics and affinity information can be obtained by tracking this shift versus time. Earlier, work by Yu et al. has shown an *in vitro* real-time monitoring of VEGF-bevacizumab binding using SPR.[34] However, the experimental conditions were not comparable to the *in vivo* VEGF−VEGFR angiogenic switch as it was performed with a commercial VEGF solution. Therefore, an alternative real-time binding kinetic study method is urgently needed to mimic the *in vivo* VEGF−VEGFR angiogenic switch for fundamental studies and drug development. In our previous study, we have successfully demonstrated real-time monitoring of VEGF expression from living human ovarian carcinoma cells using SPR.[35] By integrating a mini cell culture system into the SPR flow system, we were able to maintain live-cell culture on the ceiling of the SPR flow chamber to realize VEGF measurements from live-cells. In this study, we have measured and compared the binding affinity of VEGF to VEGFR and VEGF to bevacizumab. Finally, we employed this live-cell sensing platform to mimic the *in vivo* condition of the VEGF−VEGFR angiogenic switch. The results demonstrated a significant blockage of VEGF−VEGFR binding by bevacizumab. With this successful prove of concept, we believe that this simple and highly sensitive biomimic platform possesses great potential in the future biomolecular binding studies and drug evaluation.

EXPERIMENTAL SECTION

Reagents. 11-Mercaptoundecanoic acid (MUA) was purchased from Asemblon (Redmond, WA). Calcium ionophore (A23187) and Kreb's buffer were from Sigma-Aldrich (St. Louis, MO). 1-Ethyl-3-(3-dimethylaminopro-pyl) carbodiimidehydrochloride (EDC) and *N*-hydroxysuccinamide (NHS) were obtained from Alfa Aesar (Ward Hill, MA). Bevacizumab was kindly donated by Genentech (San Francisco, CA). Recombinant human VEGF and VEGFR were purchased from R&D Systems (Minneapolis, MN).

Cell Culture and Viability Test. In order to maintain cell viability during the measurements, a customized polydimethylsiloxane (PDMS) SPR flow chamber gasket was treated by applying several drops of 0.1% w/v gelatin solution made with boiling distilled water to cover the entire surface and dried for 12 h. A cell culture Petri dish and an uncoated PDMS gasket were also prepared and employed as positive and negative control substrates, respectively. SKOV-3 cells were cultured in McCoy's 5A medium added with 1% penicillin and 10% fetal bovine serum and kept in a 37 °C cell incubator maintained with a humidified atmosphere of 5% CO_2 and 95% air. A total of 200 000 cells were seeded on each substrate and kept with cell culture media for 48 h before experiments. Cell viability on each substrate was evaluated using a previously reported fluorescent imaging method[35] (described in the Supporting Information).

Functionalization of the SPR Sensing Surface. Carboxylic groups were immobilized on the gold SPR chip (Biosensing Instrument, AZ) by incubation in 1 mM MUA/ethanol solution for 12 h at 4 °C. The SPR chip was then washed with copious ethanol and mounted on the SPR instrument (described in the Supporting Information). After starting the flowing buffer, a solution of 75 mM EDC and 15 mM NHS in water was injected into the flowing buffer to activate the carboxylic groups. Following this, 50 μg/mL of protein G solution was injected to cover the activated SPR chip to ensure proper antibody orientation. All injections in this study were performed with a 20 μL/min rate unless otherwise specified.

Living Cell Integration to the SPR System. The flowing PBS buffer was stopped immediately after the SPR chip functionalization and the immobilization of ligands. The PDMS gasket in the SPR flow chamber used for surface immobilization (no cells) was changed to the PDMS gasket with cells, and SPR flowing buffer was changed from PBS (pH = 7.4) to Kreb's buffer (pH = 7.4) in order to maintain the cell viability during experiments. The PDMS flow chamber gasket with SKOV-3 cell culture was removed from cell culture media and thoroughly rinsed with Kreb's buffer to remove cell culture media and unattached cells before mounting on the SPR flow chamber for measurements. As shown in Scheme 1, living cells

Scheme 1. Schematic Illustration of the Biomimic System for Bevacizumab Drug Regulation Study

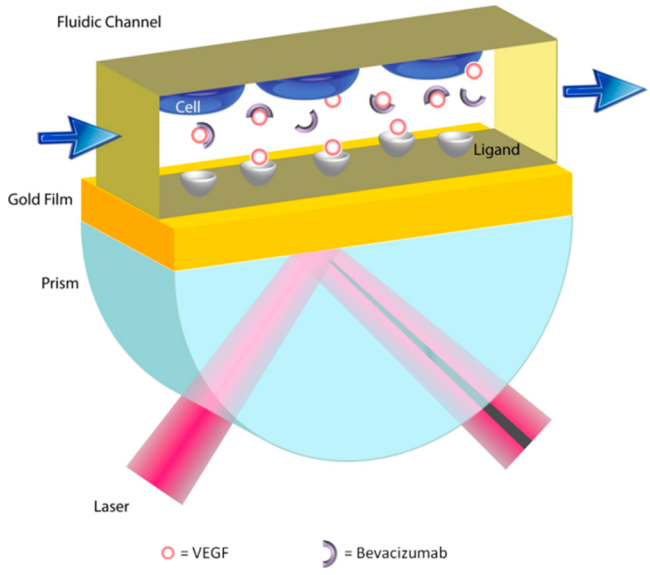

dx.doi.org/10.1021/ac402659j | *Anal. Chem.* 2014, 86, 7305−7310

are attached on the ceiling of a customized SPR flow cell chamber; VEGFR is immobilized on the SPR chip. A chemical stimulation is used to induce the rapid secretion of VEGF from cells. Bevacizumab is added to the system to actively block the VEGF−VEGFR angiogenic switch. Competitive binding to VEGF between VEGFR and bevacizumab was monitored in real-time.

RESULTS AND DISCUSSION

Cell Viability in the SPR Flow Chamber. As shown in Figure 1, the cell count within the same area on the tissue culture plate, the gelatin coated gasket, and the uncoated gasket are found to be 166 ± 8 (n = 3), 227 ± 10 (n = 3), and 79 ± 7 (n = 3), respectively. With a significant enhancement of cell attachment compared to uncoated gaskets, gelatin coated gaskets were demonstrated to be a suitable substrate to maintain the cell viability for live-cell experiments in the SPR flow chamber.[36]

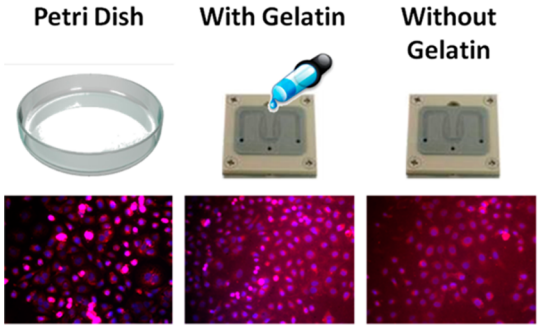

Figure 1. Merged fluorescent images (Hoechst channel & MitoTracker Red channel) of SKOV-3 cells on different type of substrates: Petri dishes (exposure time 400 ms), gelatin coated gaskets (exposure time 200 ms), and uncoated gaskets (exposure time 200 ms).

Optimization of Bevacizumab Dosing. In order to determine the optimal dose of bevacizumab for this study, we have investigated the SPR response corresponding to various amounts of bevacizumab immobilized on the gold sensing surface. Initially, a known concentration of bevacizumab (5 μg/mL, 10 μg/mL, 30 μg/mL, 50 μg/mL, 70 μg/mL) was injected to the functionalized SPR chip. A solution of 3 μg/mL VEGF (recombinant, Sigma-Aldrich) was then injected to pass through the sensing surface. The SPR measurement was repeated three times for every single bevacizumab concentration. Figure 2 shows the results corresponding to one set of measurements. The resulting SPR response for each bevacizumab concentration was plotted against time (70 μg/mL data not shown). It is evident that the amount of VEGF bound to the 50 μg/mL bevacizumab sensing surface did not show a significant difference than the amount of VEGF bound to the 30 μg/mL bevacizumab sensing surface (Figure 2). This observation can be attributed to the following two possible reasons: (i) 30 μg/mL is the saturation concentration of bevacizumab on the surface or (ii) 3 μg/mL VEGF injection can be completely captured by 30 μg/mL surface bound bevacizumab. Our previous study indicated that even if SKOV-3 cells reached 100% confluency in the SPR flow chamber, the VEGF release did not reach 3 μg/mL.[35] Therefore, the dynamic range of the sensor employed in this work is suitable for the live-cell measurements. We employed 30 μg/mL of bevacizumab as the optimum concentration for further binding studies.

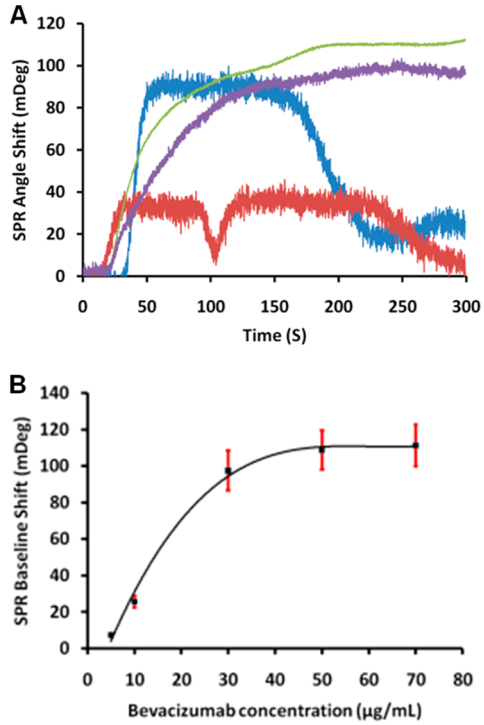

Figure 2. (A) SPR response corresponding to 3 μg/mL VEGF for each surface bound bevacizumab concentration: 5 μg/mL (red), 10 μg/mL (blue), 30 μg/mL (purple), 50 μg/mL (green); (B) SPR baseline shift induced by each different surface concentration of bevacizumab (n = 3): 8.5 ± 1.3 (5 μg/mL), 26.1 ± 3.6 (10 μg/mL), 96.1 ± 9.8 (30 μg/mL), 107.2 ± 9.3 (50 μg/mL), 111.6 ± 11.2 (70 μg/mL).

Specificity Study of VEGF-Bevacizumab Binding. Bevacizumab is a humanized anti-VEGF monoclonal antibody generated by engineering the VEGF binding residues of a murine neutralizing antibody into the framework of the human IgG.[37] Any nonspecific binding to other biomolecules is expected to affect the efficacy of this drug. Earlier, we have demonstrated the affinity and reproducibility of VEGF-bevacizumab binding. In this experiment, we further investigated the specificity of the VEGF-bevacizumab interaction. VEGF−VEGFR binding and activation is the most important step of the angiogenesis process, which is also the target of most angiogenesis regulation therapy strategies, including bevacizumab.[38,39] Thus, it is crucial to investigate the interaction between bevacizumab and VEGFR. Similarly, a bevacizumab layer was formed on the activated SPR gold surface by injecting 10 μg/mL of bevacizumab. Following this, 3 μg/mL VEGF and VEGFR were injected and passed the two bevacizumab covered gold chips, respectively. As shown in Figure 3A, a 25.1 mDeg baseline shift was observed in the SPR sensogram upon comparing the stable baseline positions before and after the injection. Such a baseline shift can be attributed to the VEGF-bevacizumab binding. However, no significant baseline shift was detected for the VEGFR−bevacizumab interaction (Figure 3B). From the results, it is evident that bevacizumab competitively binds with VEGF and thereby minimizes the amount of VEGF available to the VEGF−VEGFR interaction.

dx.doi.org/10.1021/ac402659j | Anal. Chem. 2014, 86, 7305−7310

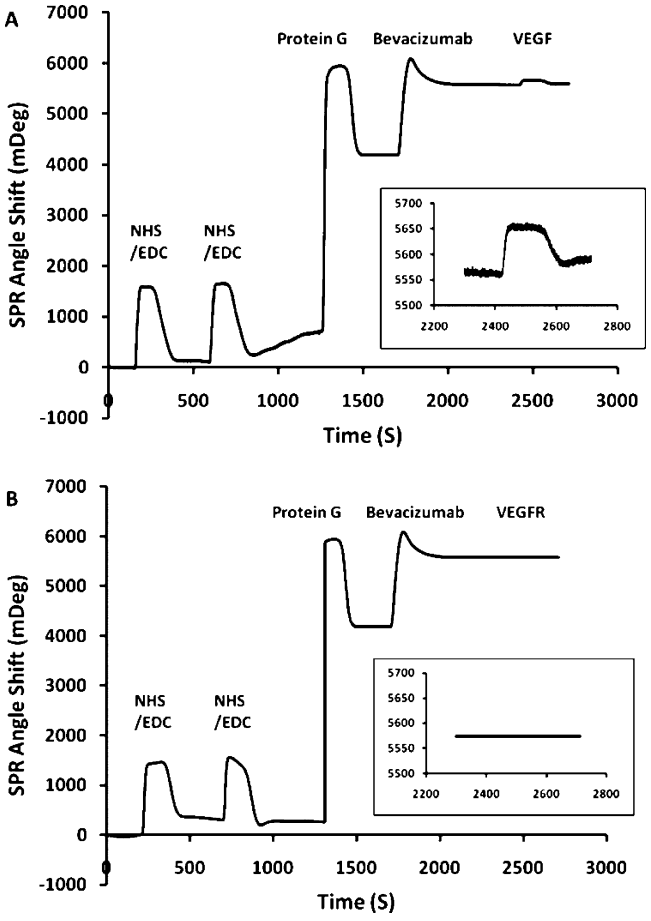

Figure 3. (A) SPR sensorgram of surface bound bevacizumab interacting with VEGF. Inset: enlarged sensorgram of the response upon VEGF binding. (B) SPR sensorgram of surface bound bevacizumab interacting with VEGFR. Inset: enlarged sensorgram of the response upon VEGFR binding.

Binding Kinetics Study of VEGF–VEGFR and VEGF–Bevacizumab Interactions. To demonstrate the drug efficacy of bevacizumab, binding kinetics of VEGF–VEGFR and VEGF–bevacizumab interactions was measured and compared. After the surface activation and modification of the SPR gold chip, 30 μg/mL of bevacizumab was immobilized on top of the protein G layer. Another SPR chip was immobilized by direct injection of 30 μg/mL of VEGFR onto the activated surface without the protein G layer. A solution of 2 μg/mL VEGF was injected to the flow chamber after surface functionalization. The SPR sensorgram corresponding to the responses on VEGF binding to bevacizumab (blue) and VEGFR (red) is shown in Figure 4A. A modified pseudo-first-order kinetics equation[40] was used to determine the association rate constants (described in Supporting Information):

$$\frac{dR}{dt} = \mathrm{ka}[\mathrm{VEGF}]\mathrm{Rmax}$$

where R is the SPR signal at time t, ka is the association rate constant which indicates the binding affinity between two molecules, [VEGF] is the concentration of VEGF, and Rmax is the maximum response of the immobilized ligand (bevacizumab or VEGFR). The value of (dR/dt) for each sample was determined by calculating the maximum slope of the association curve using Matlab 7.1 (SP3). The weight concentration of VEGF was converted to molar concentration (47.6 nM). The maximum SPR response of the surface bound bevacizumab is 1321 mDeg and the ka for bevacizumab is 1.45 $\pm$ 0.05 $\times$ 10^5 M^{-1} s^{-1} (n = 3) (repeated trails, 1.63 $\pm$ 0.06 $\times$ 10^5 M^{-1} s^{-1}; 1.41 $\pm$ 0.05 $\times$ 10^5 M^{-1} s^{-1}). Similarly, the maximum SPR response of the surface bound VEGFR is 1078 mDeg, the ka for VEGFR is 0.83 $\pm$ 0.03 $\times$ 10^5 M^{-1} s^{-1} (n = 3) (repeated trails, 0.91 $\pm$ 0.04 $\times$ 10^5 M^{-1} s^{-1}; 0.82 $\pm$ 0.03 $\times$ 10^5 M^{-1} s^{-1}). We also obtained the binding affinity information for both interactions from Figure 4A by measuring the SPR baseline shift upon VEGF binding. VEGF–bevacizumab binding induced a 92.7 $\pm$ 4 mDeg baseline shift (repeated trails, 106.5 $\pm$ 6 mDeg; 89.8 $\pm$ 3 mDeg), whereas VEGF–VEGFR binding induced a 60.2 $\pm$ 3 mDeg baseline shift (repeated trails, 69.3 $\pm$ 3 mDeg; 57.4 $\pm$ 2 mDeg). Results of ka and SPR baseline shift from three similar experiments with different batch of SKOV-3 cells are shown in parts B and C of Figure 4, respectively. Each experiment was repeated three times with intertrail coefficient of variation (CV) ranging from 0.034 to 0.056. These results indicate that bevacizumab binds VEGF with a higher rate and affinity compared to VEGFR.

Biomimic Drug Regulation Study on VEGF–VEGFR Interaction. The biomimic system was employed to evaluate the bevacizumab drug regulation on the VEGF angiogenic switch. VEGFR was immobilized on the SPR gold sensing surface by the aforementioned method. The PDMS gasket with living cells was then integrated to the SPR system. After restarting the experiment, 500 μm Ca^{2+} ionophore (A23187)

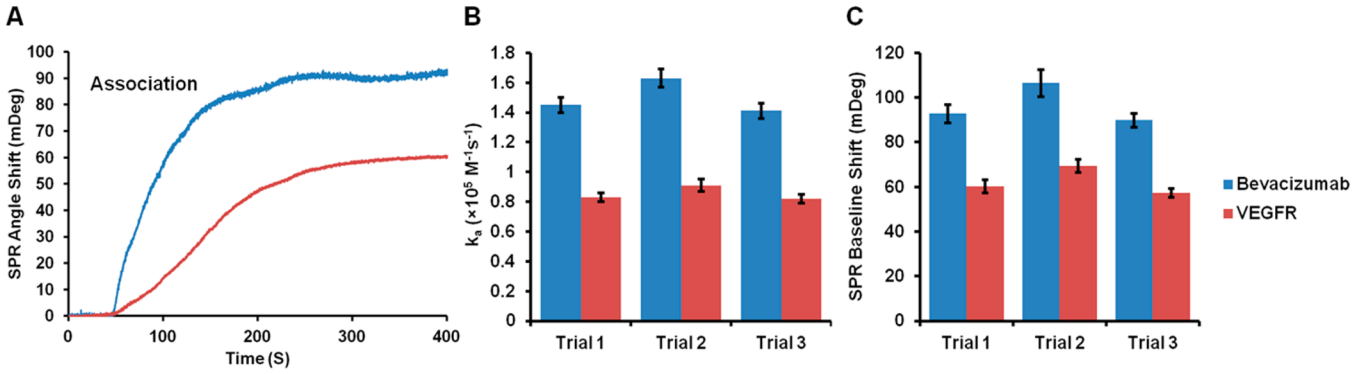

Figure 4. (A) SPR sensorgram of VEGF binding response to bevacizumab (blue line) and VEGFR (red line). (B) Association rate constants (ka) of VEGF–bevacizumab binding (blue) and VEGF–VEGFR binding (red) calculated for each trial of experiment. (n = 3). (C) Binding affinity indicated by SPR baseline shift of VEGF–bevacizumab binding (blue) and VEGF–VEGFR binding (red) for each trial (n = 3).

dx.doi.org/10.1021/ac402659j | Anal. Chem. 2014, 86, 7305–7310

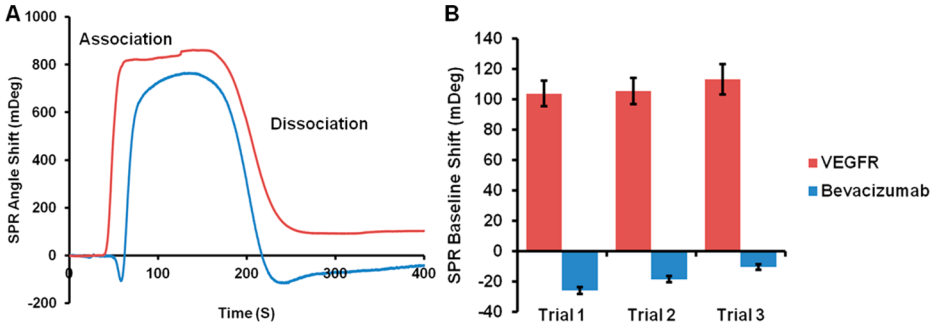

Figure 5. (A) SPR response of VEGF (SKOV-3 cells released)−VEGFR interaction (red line) and VEGF (SKOV-3 cells released)−VEGFR interaction under bevacizumab regulation (blue line) in the biomimic system. (B) SPR baseline shift of VEGF−VEGFR interaction (red) and VEGF−VEGFR interaction under bevacizumab regulation (blue) for each trial. (n = 3).

was injected to induce rapid exocytosis of VEGF from the SKOV-3 cells.[29] In Figure 5A, the red line represents the SPR response of VEGF exocytosis binding to VEGFR on the sensing surface (control experiment). The peak between ∼50 s and ∼250 s is attributed to the refractive index change induced by the Ca^{2+} ionophore (A23187) passing through the sensing surface. Following the plateau, the baseline is stabilized at 103.7 ± 8 mDeg (repeated trails, 105.6 ± 9 mDeg, 113.2 ± 10 mDeg). This SPR baseline shift indicates that VEGF released from SKOV-3 cells has bound to the VEGFR. The blue line depicts the SPR response of VEGF exocytosis binding to surface VEGFR under the regulation of bevacizumab (drug regulation experiment). A solution of 30 μg/mL bevacizumab was added to the flowing buffer to bind the VEGF secretion in this group. This data, upon comparison with the control experiment, has shown that the SPR baseline dropped by 82.5 ± 9.6 mDeg after the Ca^{2+} ionophore (A23187) stimulation. Similar results were observed in experiments with different batch of SKOV-3 cells. We anticipate this sudden drop of baseline as a result of the surface refractive index decrease caused by the rapid binding event occurred between VEGF and bevacizumab in the flowing buffer. However, further experiments are essential to validate this assumption. Following the plateau, the baseline slowly increased toward the original position to −25.8 ± 2 mDeg (repeated trails, −18.4 ± 2 mDeg; −10.5 ± 2 mDeg) as a consequence of the VEGF exocytosis being carried away from the sensing surface. No significant baseline increase was observed after the induced exocytosis, thereby confirming that the VEGF−VEGFR pathway was successfully blocked by bevacizumab in the flow chamber. Figure 5B shows the SPR baseline shift with and without bevacizumab regulation obtained from three similar experiments with different batch of SKOV-3 cells. Each experiment was repeated three times with intertrail CV ranging from 0.081 to 0.18. These results indicate that the amount of VEGF bound to VEGFR was significantly decreased under the regulation of bevacizumab.[41]

CONCLUSION

In summary, we have constructed a biomimic system for the VEGF−VEGFR angiogenic switch in SPR and investigated its potential application on antineoplastic drugs development. To the best of our knowledge, this is the first report showing direct and real-time measurements of drug effect to the VEGF−VEGFR angiogenic switch on live-carcinoma cells. SKOV-3 cells and the bevacizumab antibody were used as the cell model and the drug model to evaluate the strategy. SPR exhibited excellent sensitivity and linear dynamic range toward VEGF and bevacizumab interactions. VEGF−bevacizumab binding indicated a higher association rate constant and binding affinity than VEGF−VEGFR binding. The bevacizumab drug regulation study reveals successful blockage of VEGF−VEGFR binding and activation process. We have outlined a highly sensitive and simple strategy for the direct and real-time measurements of bevacizumab drug efficacy to the VEGF−VEGFR angiogenic switch on living SKOV-3 cells. A similar strategy can be adopted to develop and evaluate other types of medicine in the future.

ASSOCIATED CONTENT

Supporting Information

Additional information as noted in text. This material is available free of charge via the Internet at http://pubs.acs.org.

AUTHOR INFORMATION

Corresponding Author

*E-mail: licz@fiu.edu.

Notes

The authors declare no competing financial interest.

ACKNOWLEDGMENTS

This study was supported by the Grant R15ES021079 from the National Institutes of Health (USA), Grant 1334417 from the National Science Foundation (NSF), and Grant 21328501 from the National Natural Science Foundation of China to Prof. Chen-Zhong Li. Dr. Subbiah Alwarappan acknowledges Director Dr. Vijayamohanan K. Pillai, CSIR-CECRI for the startup grant, Grant OLP 0088, awarded to him. The authors thank Genentech, Inc. (San Fransisco, CA) for providing bevacizumab free of cost.

REFERENCES

(1) Siegel, R.; Naishadham, D.; Jemal, A. *CA Cancer J. Clin.* **2012**, *62*, 10−29.
(2) Reya, T.; Morrison, S. J.; Clarke, M. F.; Weissman, I. L. *Nature* **2001**, *414*, 105−111.
(3) Heng, H. H. Q.; Stevens, J. B.; Bremer, S. W.; Ye, K. J.; Liu, G.; Ye, C. J. *J. Cell. Biochem.* **2010**, *109*, 1072−1084.
(4) Mantovani, A.; Allavena, P.; Sica, A.; Balkwill, F. *Nature* **2008**, *454*, 436−444.
(5) Kerbel, R. S. *N. Engl. J. Med.* **2008**, *358*, 2039−2049.
(6) Hanahan, D.; Weinberg, R. A. *Cell* **2011**, *144*, 646−674.
(7) Risau, W. *Nature* **1997**, *386*, 671−674.
(8) Carmeliet, P. *Nat. Med.* **2000**, *6*, 389−395.
(9) Carmeliet, P.; Jain, R. K. *Nature* **2000**, *407*, 249−257.

(10) Bergers, G.; Benjamin, L. E. *Nat. Rev. Cancer* **2003**, *3*, 401−410.
(11) Neufeld, G.; Cohen, T.; Gengrinovitch, S.; Poltorak, Z. *FASEB J.* **1999**, *13*, 9−22.
(12) Hicklin, D. J.; Ellis, L. M. *J. Clin. Oncol.* **2005**, *23*, 1011−1027.
(13) Longo, R.; Sarmiento, R.; Fanelli, M.; Capaccetti, B.; Gattuso, D.; Gasparini, G. *Angiogenesis* **2002**, *5*, 237−56.
(14) Ferrara, N.; Kerbel, R. S. *Nature* **2005**, *438*, 967−974.
(15) Prewett, M.; Huber, J.; Li, Y. W.; Santiago, A.; O'Connor, W.; King, K.; Overholser, J.; Hooper, A.; Pytowski, B.; Witte, L.; Bohlen, P.; Hicklin, D. J. *Cancer Res.* **1999**, *59*, 5209−5218.
(16) Badr, H.; ElSayed, A.; Ahmed, H.; Dwek, M.; Li, C.-z.; Djansugurova, L. *Appl. Biochem. Biotechnol.* **2013**, *171*, 963−974.
(17) Presta, L. G.; Chen, H.; Oconnor, S. J.; Chisholm, V.; Meng, Y. G.; Krummen, L.; Winkler, M.; Ferrara, N. *Cancer Res.* **1997**, *57*, 4593−4599.
(18) Ferrara, N.; Hillan, K. J.; Gerber, H. P.; Novotny, W. *Nat. Rev. Drug Discovery* **2004**, *3*, 391−400.
(19) Fuh, G.; Wu, P.; Liang, W. C.; Ultsch, M.; Lee, C. V.; Moffat, B.; Wiesmann, C. *J. Biol. Chem.* **2006**, *281*, 6625−6631.
(20) Johnson, D. H.; Fehrenbacher, L.; Novotny, W. F.; Herbst, R. S.; Nemunaitis, J. J.; Jablons, D. M.; Langer, C. J.; DeVore, R. F.; Gaudreault, J.; Damico, L. A.; Holmgren, E.; Kabbinavar, F. *J. Clin. Oncol.* **2004**, *22*, 2184−2191.
(21) Miller, K. D.; Chap, L. I.; Holmes, F. A.; Cobleigh, M. A.; Marcom, P. K.; Fehrenbacher, L.; Dickler, M.; Overmoyer, B. A.; Reimann, J. D.; Sing, A. P.; Langmuir, V.; Rugo, H. S. *J. Clin. Oncol.* **2005**, *23*, 792−799.
(22) Saltz, L. B.; Clarke, S.; Diaz-Rubio, E.; Scheithauer, W.; Figer, A.; Wong, R.; Koski, S.; Lichinitser, M.; Yang, T. S.; Rivera, F.; Couture, F.; Sirzen, F.; Cassidy, J. *J. Clin. Oncol.* **2008**, *26*, 2013−2019.
(23) Friedman, H. S.; Prados, M. D.; Wen, P. Y.; Mikkelsen, T.; Schiff, D.; Abrey, L. E.; Yung, W. K. A.; Paleologos, N.; Nicholas, M. K.; Jensen, R.; Vredenburgh, J.; Huang, J.; Zheng, M. X.; Cloughesy, T. *J. Clin. Oncol.* **2009**, *27*, 4733−4740.
(24) Tol, J.; Koopman, M.; Cats, A.; Rodenburg, C. J.; Creemers, G. J. M.; Schrama, J. G.; Erdkamp, F. L. G.; Vos, A. H.; van Groeningen, C. J.; Sinnige, H. A. M.; Richel, D. J.; Voest, E. E.; Dijkstra, J. R.; Vink-Borger, M. E.; Antonini, N. F.; Mol, L.; van Krieken, J.; Dalesio, O.; Punt, C. J. A. *N. Engl. J. Med.* **2009**, *360*, 563−572.
(25) McDermott, D. F.; George, D. J. *Cancer Treat. Rev.* **2010**, *36*, 216−223.
(26) Yang, J. C.; Haworth, L.; Sherry, R. M.; Hwu, P.; Schwartzentruber, D. J.; Topalian, S. L.; Steinberg, S. M.; Chen, H. X.; Rosenberg, S. A. *N. Engl. J. Med.* **2003**, *349*, 427−434.
(27) Bock, F.; Onderka, J.; Dietrich, T.; Bachmann, B.; Kruse, F. E.; Paschke, M.; Zahn, G.; Cursiefen, C. *Invest. Ophthalmol. Vis. Sci.* **2007**, *48*, 2545−2552.
(28) Klettner, A.; Roider, J. *Invest. Ophthalmol. Vis. Sci.* **2008**, *49*, 4523−4527.
(29) Prabhulkar, S.; Alwarappan, S.; Liu, G.; Li, C.-Z. *Biosens. Bioelectron.* **2009**, *24*, 3524−3530.
(30) Zhu, X.; Hondroulis, E.; Liu, W.; Li, C.-Z. *Small* **2013**, *9*, 1821−1830.
(31) Li, Y.; Lee, H. J.; Corn, R. M. *Anal. Chem.* **2007**, *79*, 1082−1088.
(32) Cochran, S.; Li, C. P.; Fairweather, J. K.; Kett, W. C.; Coombe, D. R.; Ferro, V. *J. Med. Chem.* **2003**, *46*, 4601−4608.
(33) Li, C.-Z.; Vandenberg, K.; Prabhulkar, S.; Zhu, X.; Schneper, L.; Methee, K.; Rosser, C. J.; Almeide, E. *Biosens. Bioelectron.* **2011**, *26*, 4342−4348.
(34) Yu, L. L.; Wu, X. M.; Cheng, Z. Y.; Lee, C. V.; LeCouter, J.; Campa, C.; Fuh, G.; Lowman, H.; Ferrara, N. *Invest. Ophthalmol. Vis. Sci.* **2008**, *49*, 522−527.
(35) Liu, C.; Lei, T.; Ino, K.; Matsue, T.; Tao, N.; Li, C.-Z. *Chem. Commun.* **2012**, *48*, 10389−10391.
(36) Liu, H. C.; Ito, Y. *Lab Chip* **2002**, *2*, 175−178.
(37) Kramer, I.; Lipp, H. P. *J. Clin. Pharm. Ther.* **2007**, *32*, 1−14.
(38) Plate, K. H.; Scholz, A.; Dumont, D. J. *Acta Neuropathol.* **2012**, *124*, 763−775.
(39) Ziche, M.; Donnini, S.; Morbidelli, L. *Curr. Drug Targets* **2004**, *5*, 485−493.
(40) Edwards, P. R.; Leatherbarrow, R. J. *Anal. Biochem.* **1997**, *246*, 1−6.
(41) Nagengast, W. B.; de Vries, E. G.; Hospers, G. A.; Mulder, N. H.; de Jong, J. R.; Hollema, H.; Brouwers, A. H.; van Dongen, G. A.; Perk, L. R.; Lub-de Hooge, M. N. *J. Nucl. Med.* **2007**, *48*, 1313−1319.